Bose-Glass Phases in Disordered Quantum Magnets

Omid Nohadani,[1] Stefan Wessel,[2] and Stephan Haas[1]

[1]*Department of Physics and Astronomy, University of Southern California, Los Angeles, California 90089-0484, USA*
[2]*Institut für Theoretische Physik III, Universität Stuttgart, 70550 Stuttgart, Germany*

(Received 26 May 2005; published 21 November 2005)

In disordered spin systems with antiferromagnetic Heisenberg exchange, transitions into and out of a magnetic-field-induced ordered phase pass through unique regimes. Using quantum Monte Carlo simulations to study the zero-temperature behavior, these intermediate regions are determined to be Bose-glass phases. The localization of field-induced triplons causes a finite compressibility and, hence, glassiness in the disordered phase.

DOI: 10.1103/PhysRevLett.95.227201 PACS numbers: 75.10.Nr, 73.43.Nq, 75.50.Ee, 75.50.Lk

Bose-glass phenomena have recently been reported in a variety of disordered quantum many-body systems, including trapped atoms, vortex lattices, and Heisenberg antiferromagnets. These experiments have in common signatures of finite compressibility in proximity to a Bose-Einstein condensate. In atomic waveguides, the fragmentation of such a condensate is caused by a random modulation of the local atomic density [1]. It was shown that a quantum phase transition between the superfluid and the insulating Bose-glass phases can be achieved under realistic experimental conditions [2]. Furthermore, recent transport measurements of vortex dynamics in high-temperature superconducting cuprates have shown evidence of a Bose-glass transition [3]. In the context of quantum antiferromagnetism, recent measurements of the magnetization and the specific heat have suggested a glassy regime in proximity to a magnetic-field-induced triplon condensate [4,5]. However, a theoretical understanding of the Bose-glass phenomena in quantum spin systems based on a microscopic Hamiltonian is still lacking.

In this Letter, we study how disorder affects the quantum phase transition between a valence bond solid and a magnetic-field-induced Néel-ordered phase in an antiferromagnetic Heisenberg spin system. Using large-scale quantum Monte Carlo simulations down to ultralow temperatures, we observe that, in cubic dimer systems with bond randomness, there is an intermediate Bose-glass regime, separating an antiferromagnetically ordered phase of condensed triplons from a spin liquid phase of localized triplons at low magnetic fields. For weak interdimer couplings, this model can be mapped onto a lattice boson model with random potential [6]. The Néel-ordered phase of delocalized triplons corresponds to the superfluid regime in the bosonic language. It is characterized by a finite staggered magnetization perpendicular to the applied magnetic field $m_s^{\perp}$, analogous to the superfluid order parameter in a bosonic system. The Bose-glass phase is distinguished by a finite slope of the uniform magnetization m_u as a function of the applied magnetic field, i.e., compressible bosons, whereas the order parameter $m_s^{\perp}$ vanishes.

In order to probe these observables and, thus, study emerging quantum phase transitions in such disordered quantum magnets, we apply the stochastic series expansion (SSE) quantum Monte Carlo (QMC) method [7]. In particular, the directed-loop algorithm is used to minimize bounce probabilities in the loop construction when magnetic fields are applied to the system [8]. Ultralow temperatures are chosen such that the relevant thermodynamic observables reflect true zero-temperature behavior. In this work, we apply SSE QMC to a dimerized antiferromagnetic spin-1/2 Heisenberg model on a cubic lattice,

$$H = \sum_{\langle i,j \rangle} J_{ij} \mathbf{S}_i \cdot \mathbf{S}_j - h \sum_i S_i^z, \tag{1}$$

where h denotes the external magnetic field. The dimers are aligned along the x direction with the intradimer coupling $J_{ij} = J$. They are linked with each other via interdimer couplings $J_{ij} = J'$ in all three spatial directions, as shown in Fig. 2(a). Disorder is introduced in the intradimer couplings, which can take values $J = J_1$ or $J = J_2$ according to a bimodal distribution $P(J, x) = (1 - x) \times \delta(J - J_1) + x\delta(J - J_2)$ and doping concentration x with $J_1 > J_2$. Typically, up to 500 disorder realizations are included in the statistics for $L \leq 16$ and $8 \times 10^3/L$ for larger system sizes.

The order parameter $m_s^{\perp}$ can be calculated from the staggered structure factor,

$$S_s^{\perp} = \frac{1}{L^3} \sum_{\langle i,j \rangle} (-1)^{i+j} \langle S_i^x S_j^x \rangle, \quad \text{as } m_s^{\perp} = \sqrt{\frac{S_s^{\perp}}{L^3}}, \tag{2}$$

where L denotes the size of the system.

Figure 1 shows m_u and $m_s^{\perp}$ as a function of the applied magnetic field for $J_1 = 2J_2 = 10J'$ and $x = 0.1$. A rich field dependence is observed. For $h \geq 0.75J_1$, the singlet-triplet gap closes and m_u increases with the magnetic field. The observed linear dependence on the applied field is expected from the XY universality class [9]. Furthermore, the external field induces a finite magnetic moment perpendicular to the field direction, $m_s^{\perp}$ [10]. A square-root

increase of $m_s^\perp$ is observed, indicating a field-induced Bose-Einstein condensation (BEC) of triplons, which extends up to the saturation field. At higher fields ($h \geq 1.5J_1$), all spins polarize fully along the field direction. Zooming into the field region smaller than $0.75J_1$ reveals a small bump in $m_s^\perp$. For finite system sizes, $m_s^\perp$ is inversely proportional to the system length L close to the lower critical field [9]. The inset in Fig. 1(a) shows $m_s^\perp$ for two field strengths, extrapolated to the thermodynamic limit. While the offset vanishes for small fields, the small bump around $h = 0.54J_1$ remains finite as $L \to \infty$, indicating an ordered phase of delocalized triplons from the doped bonds, which undergo a BEC. Figure 1(b) is a magnification of the interesting field region around this bump. It also contains extrapolated data. They reveal that, for $0.44J_1 \leq h \leq 0.5J_1$, the order parameter vanishes, whereas the uniform magnetization has a finite slope. This signifies a new, disorder-induced phase prior to the BEC.

Since the interdimer coupling is chosen much smaller than both intradimer couplings, this system can be mapped onto a hard-core boson model with a random potential as sketched in Fig. 1(c). Deeper potential dips occur at random positions, reflecting that some of the intradimer couplings are weaker. The chemical potential μ, corresponding to the applied magnetic field, governs the occupation of hard-core bosons in the potential dips. At small μ, only the lowest minima are filled, and those spatially closer to each other cause islands of localized bosons. The finite slope of the magnetization in Fig. 1(b) indicates a finite compressibility of the triplons in this picture. Hence, in the region next to the BEC phase, the system is compressible but not ordered because of triplon localization. This is the manifestation of a Bose-glass phase. The more islands of compressible bosons that are created, the larger the probability for the islands to come closer to each other. Hence, there are enhanced correlations between the triplons due to the background interaction of the undoped bonds. The localization disappears as soon as this interaction becomes relevant, which occurs at the BEC transition. Therefore, each transition between the Mott-insulating and the superfluid phases should pass through a Bose-glass regime [6]. This study delivers the first numerical evidence for the existence of a Bose-glass phase in a microscopic spin model.

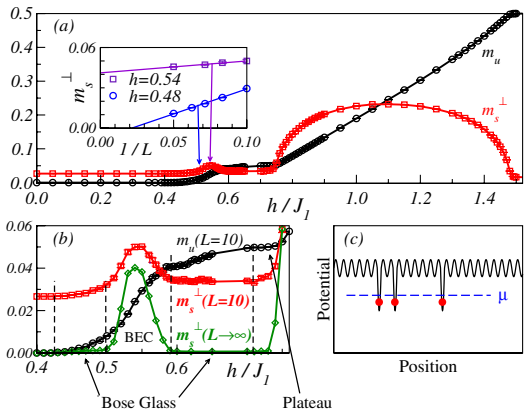

FIG. 1 (color online). (a) Zero-temperature uniform and transverse staggered magnetization as a function of field for intradimer couplings $J_1 = 2J_2$, interdimer coupling $J' = 0.1J_1$, and doping concentration $x = 0.1$ for $10 \times 10 \times 10$ spins. (b) Magnification of the "minicondensation" surrounded by two neighboring Bose-glass phases, in which m_u has a finite slope, whereas $m_s^\perp$ vanishes. m_u exhibits a plateau at the doping fraction of full polarization. The quantum phase transition beyond the plateau is a Bose-Einstein condensation of triplons on the stronger dimer bonds. The effective bosonic random potential is illustrated in (c), where the magnetic field corresponds to the chemical potential μ, which controls the bosons (circles).

Figure 2 provides a schematic picture of the different phases observed in the QMC data. Planar sections of the cubic lattice are shown, containing weakly coupled spin dimers. In the clean case and at sufficiently small fields, the dimer valence bond solid is energetically the lowest state, as shown in Fig. 2(a). The quantum phase transition at the lower critical field may be regarded as a BEC of magnons in the lowest triplet branch. Ultimately, at the upper critical field, all spins align fully along the field direction. In the randomly doped case, Fig. 2(b) shows seven possible phases. The dimer valence bond solid is the ground state at small fields (region I). It requires a finite magnetic field

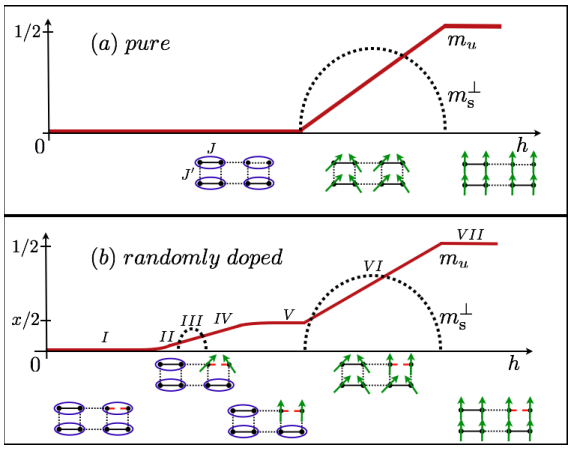

FIG. 2 (color online). Schematic response of the zero-temperature uniform and staggered magnetizations to an applied magnetic field. Within the planes of the cubic lattice, dotted lines denote interdimer couplings J' and solid lines the intradimer couplings. At small fields, the weakly coupled dimers form a valence bond solid state (elliptic bonds). In the pure case (a), Bose-Einstein condensation occurs at the lower critical field. At the saturation field, all spins are fully polarized; the system undergoes another BEC transition. For the doped case (b), intradimer bonds J take the values $J = J_1$ (solid lines) or $J = J_2$ (dashed lines). A field scan reveals the following phases: region I, valence bond solid; region II, Bose-glass phase; region III, minicondensation; region IV, another Bose-glass phase; region V, an intermediate plateau at $m_u = x \cdot m_u^{\text{sat}}$; region VI, BEC; region VII, full polarization.

strength to overcome the lowest singlet-triplet gap. Since the doped bonds are weaker ($J_2 < J_1$), these dimers break first. Their spins respond to the increasing field, leading to a finite slope of uniform magnetization as a function of the applied field. In the bosonic picture, this implies a finite compressibility of the field-induced triplons on the doped dimer bonds. These triplons are localized, and the absence of phase coherence causes $m_s^{\perp} = 0$. Region II in Fig. 2(b) illustrates this Bose-glass phase. Upon further increasing the magnetic field, delocalization of triplons sets in as they undergo a BEC transition, with $m_s^{\perp} > 0$ as in region III. In Fig. 1(b), this phase occurs in the interval $0.5J_1 \leq h \leq 0.59J_1$, where the triplons on the doped bonds interact with each other via an exponentially small effective hopping term on the background of the remaining bonds ($J'_{\text{eff}} \ll J'$) [11]; i.e., the triplons become delocalized. In the bosonic picture, this ordered regime is the superfluid phase. Upon further increasing the field, the spins align progressively along the field direction. Eventually, $m_s^{\perp}$ vanishes and the delocalization disappears, which constitutes another Bose-glass phase upon exiting the ordered regime. In Fig. 1(b), this occurs for $0.59J_1 \leq h \leq 0.71J_1$, corresponding to region IV in Fig. 2(b).

The glassy phase of localized triplons disappears when all the spins of the doped bonds become fully polarized. If the lower critical field of the undoped bonds $h_{c1}(J_1, J')$ is larger than the upper critical field of the doped bonds $h_{c2}(J_2, J'_{\text{eff}})$, a magnetization plateau is expected. Region II in Fig. 2(b) illustrates such a regime, in which the uniform magnetization takes a constant value of $m_u = x \cdot m_u^{\text{sat}}$. Here m_u^{sat} is the saturation magnetization and x is the doping rate. The present QMC data reveal a range of fields for which such a plateau is observed, as shown in Fig. 1(b). Moreover, it is seen that a transition into and out of the superfluid phase passes through a Bose-glass phase before entering the Mott-insulating phase; i.e., region III in Fig. 2(b) is flanked by region II and region IV before entering region I and region V, respectively. Furthermore, there are no detectable bond-disorder effects observed at and beyond the plateau, even though the fully polarized spins on the doped bonds are still randomly distributed in the system and should contribute to another Bose-glass phase after the plateau. This can be attributed to the negligible randomness effect at this level, since all of the spins on the doped bonds are saturated, both the hopping term J' and the doping rate x are small, and the doping obeys a bimodal distribution.

A further increase of the magnetic field breaks the remaining dimer singlets, as argued in region VI in Fig. 2(b), thus driving the quantum phase transition to antiferromagnetic long-range order of delocalized triplons and inducing a linear response to the magnetic field. This transition is a field-induced BEC of triplons on the bonds with strong intradimer coupling J_1. For $T > 0$, the quantum critical field strength depends on temperature as $|h - h_c| \propto T_c^{\alpha}$, where, in a narrow critical regime, α is determined to be $3/2$ [12]. This value agrees well with the mean-field prediction for BEC of bosons in the dilute limit [13]. Ultimately, at very high fields, all spins align along the field direction, and the system saturates magnetically, as illustrated in region VII in Fig. 2(b). At this threshold, another BEC with the same critical properties occurs. For this high-field transition, no Bose-glass phase is detected, as argued previously [14].

The dependence of m_u and $m_s^{\perp}$ on doping concentration and the coupling strengths are studied in Fig. 3. Different parameter sets are considered to explore the effects of bond disorder close to the quantum phase transition. The data for the doping rate $x = 0.1$ in Fig. 3(a) are the same as shown in Fig. 1. When $x = 0.9$, analogous behavior is observed for the regime $0.98J_1 \leq h \leq 1.24J_1$, due to the abundance of weaker bonds J_2. In this case, the effects of randomness, being two Bose-glass phases flanking the superfluid phase, occur as a mirror image in the vicinity of the upper critical field $h = 1.24J_1$ instead of the lower critical field $h = 0.44J_1$. A plateau with finite width occurs for $x = 0.1$, as shown in the inset in Fig. 3(a). For intermediate doping concentrations, $0.2 < x < 0.8$, the plateau is smeared out by the dimer-bond randomness. Figure 3(b) shows how the critical fields and the width of the plateau depend on the interdimer coupling J'. The plateau has its maximum extent in the limit of decoupled dimers, i.e., $J' = 0$. This width decreases with increasing interdimer coupling strength and vanishes at a critical value $J' \approx 0.15J_1$. Therefore, simulations for $J' = 0.1J_1$ reveal a finite width of the plateau as well as Bose-glass phases flanking the triplon condensate on the weaker dimer bonds. Furthermore, the ratio between the stronger and weaker intradimer bonds J_1 and J_2 controls the width of the plateau, as shown

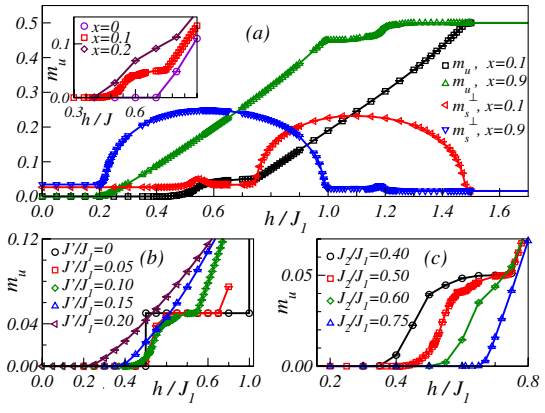

FIG. 3 (color online). Zero-temperature uniform and staggered magnetization as a function of field (a) for different doping concentrations x at $J_1 = 2J_2 = 10J'$; (b) for different interdimer couplings J' between the decoupled and strongly coupled dimer limits, with $J_1 = 2J_2$ and $x = 0.1$; (c) for different intradimer coupling strengths of the doped bonds J_2, with $J_1 = 10J'$ and $x = 0.1$.

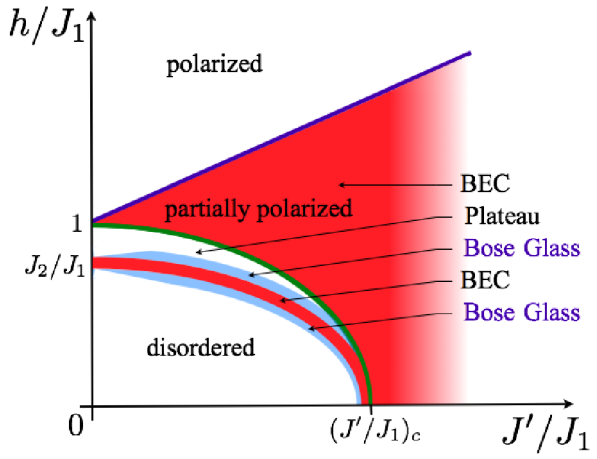

FIG. 4 (color online). Zero-temperature phase diagram of three-dimensional weakly coupled dimers with random intradimer coupling at a doping rate of $x \leq 15\%$. The plateau is most pronounced at weak interdimer couplings. For $(J'/J_1) > (J'/J_1)_c \approx 0.249$, the gap vanishes, and the order sets in at infinitesimal fields. For small x, we do not expect to detect any effects of randomness at saturation fields.

in Fig. 3(c). If the values of J_1 and J_2 are too close, the effects of randomness are suppressed, smearing out both the magnetization plateau and the Bose-glass phase. However, upon decreasing the ratio J_2/J_1, a magnetization plateau appears. A ratio of $J_2/J_1 = 1/2$ was found to be sufficiently low to clearly reveal the novel, disorder-induced quantum phases.

Indications of a Bose-glass phase between a gapped incompressible phase and a field-induced antiferromagnetic phase were recently suggested by high-field magnetization measurements on bond-disordered $Tl_{(1-x)}K_xCuCl_3$ for $x < 0.36$ [4]. More recent specific heat measurements on this compound with doping rates up to $x \leq 0.22$ examined the effect of randomness on the phase boundaries as a function of temperature. They observed the emergence of a novel phase prior to the field-induced BEC [5]. However, the linear response of the measured magnetization to the applied field starting at $h = 0$ indicates that nonmagnetic K doping of $TlCuCl_3$ not only introduces bond disorder but also a pronounced directional Dzyaloshinskii-Moriya vector [16]. Therefore, Bose-glass effects are likely to be suppressed. Hence, doped compounds with negligible spin-orbit coupling and vanishing directionality are expected to reveal Bose-glass features.

We conclude by proposing a phase diagram of weakly coupled dimers with random intradimer coupling strengths $(J_1 > J_2)$ in Fig. 4. Quantum Monte Carlo data show that, at finite randomness, a field-induced quantum phase transition into and out of an ordered Bose-Einstein condensate passes through a Bose-glass phase. The localization of the bosons and the finite compressibility manifests this unique regime. Once delocalized, the triplons condense and Néel order sets in. Depending on coupling ratios, an intermediate plateau can occur, in which the spins of the doped bonds are fully polarized. This rich field dependence is expected to be experimentally detectable in weakly coupled dimer compounds with small doping and negligible spin-orbit coupling or directionality effects.

We thank B. Normand, T. Roscilde, P. Schmidt, M. Troyer, and T. Vojta for useful discussions. Furthermore, we acknowledge financial support from DOE Award No. DE-FG02-05ER46240. S. H. and S. W. appreciate the hospitality of the Kavli Institute for Theoretical Physics. Computational support was provided by the USC High Performance Computing Center and NIC Jülich.

[1] A. E. Leanhardt *et al.*, Phys. Rev. Lett. **90**, 100404 (2003); **89**, 040401 (2002); J. Fortagh *et al.*, Phys. Rev. A **66**, 041604(R) (2002); S. Kraft *et al.*, J. Phys. B **35**, L469 (2002).
[2] D. W. Wang, M. D. Lukin, and E. Demler, Phys. Rev. Lett. **92**, 076802 (2004).
[3] L. Ammor, N. H. Hong, B. Pignon, and A. Ruyter, Phys. Rev. B **70**, 224509 (2004).
[4] A. Oosawa and H. Tanaka, Phys. Rev. B **65**, 184437 (2002).
[5] Y. Shindo and H. Tanaka, J. Phys. Soc. Jpn. **73**, 2642 (2004).
[6] M. P. A. Fisher, P. B. Weichman, G. Grinstein, and D. S. Fisher, Phys. Rev. B **40**, 546 (1989).
[7] A. W. Sandvik, Phys. Rev. B **59**, R14 157 (1999).
[8] O. F. Syljuåsen and A. W. Sandvik, Phys. Rev. E **66**, 046701 (2002); F. Alet, S. Wessel, and M. Troyer, Phys. Rev. E **71**, 036706 (2005).
[9] O. Nohadani, S. Wessel, and S. Haas, Phys. Rev. B **72**, 024440 (2005).
[10] I. Fischer and A. Rosch, cond-mat/0412284.
[11] M. Sigrist and A. Furusaki, J. Phys. Soc. Jpn. **65**, 2385 (1996).
[12] O. Nohadani, S. Wessel, B. Normand, and S. Haas, Phys. Rev. B **69**, 220402(R) (2004); S. Wessel, M. Olshanii, and S. Haas, Phys. Rev. Lett. **87**, 206407 (2001).
[13] V. N. Popov, *Functional Integrals and Collective Excitations* (Cambridge University Press, Cambridge, England, 1987); T. Giamarchi and A. M. Tsvelik, Phys. Rev. B **59**, 11 398 (1999).
[14] For $h \geq 1.5J_1$, finite-size effects are responsible for the offsets in $m_s^{\perp}$, which scales as $m_s^{\perp} = 1/\sqrt{2L^3}$ [15].
[15] O. Nohadani, S. Wessel, S. Haas, and A. Honecker (to be published).
[16] T. Moriya, Phys. Rev. **120**, 91 (1960); J. Sirker, A. Weiße, and O. P. Sushkov, Europhys. Lett. **68**, 275 (2004).